



Photoinduced and Thermal Linkage Isomerizations of an Organometallic Ionic Liquid Containing a Half-Sandwich Ruthenium Thiocyanate Complex

Mochida, Tomoyuki

Maekawa, Syou

Sumitani, Ryo

(Citation)

Inorganic Chemistry, 60(16):12386-12391

(Issue Date)

2021-08-16

(Resource Type)

journal article

(Version)

Accepted Manuscript

(Rights)

This document is the Accepted Manuscript version of a Published Work that appeared in final form in Inorganic Chemistry, copyright © American Chemical Society after peer review and technical editing by the publisher. To access the final edited and published work see <https://pubs.acs.org/articlesonrequest/AOR-MQ9IIZCH4DQQDMYRRKFN>

(URL)

<https://hdl.handle.net/20.500.14094/90009048>



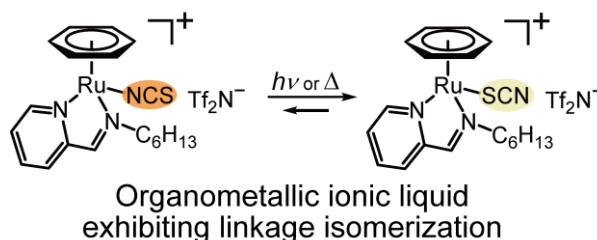
Photoinduced and Thermal Linkage Isomerizations of an Organometallic Ionic Liquid Containing a Half-Sandwich Ruthenium Thiocyanate Complex

Tomoyuki Mochida,^{*a,b} Syou Maekawa,^a and Ryo Sumitani^a

^aDepartment of Chemistry, Graduate School of Science, Kobe University, Rokkodai, Nada, Kobe, Hyogo 657-8501, Japan. E-mail: tmochida@platinum.kobe-u.ac.jp

^bResearch Center for Membrane and Film Technology, Kobe University, Rokkodai, Nada, Kobe, Hyogo 657-8501, Japan

ABSTRACT: Metal complexes with thiocyanate (SCN⁻) ligands typically exhibit *S*- or *N*-coordinated linkage isomers. In this study, to explore ionic liquids that exhibit stimuli-



responsiveness based on linkage isomerization, we synthesized an ionic liquid containing a cationic half-sandwich thiocyanate complex, [Ru(C₆H₆)(NCS)L]Tf₂N⁻ (L = *N*-hexyl-2-pyridinemethanimine, Tf₂N⁻ = bis(trifluoromethanesulfonyl)amide anion). The as-synthesized ionic liquid was a 0.7:0.3 mixture of *N*- and *S*-coordinated isomers, presenting as an extremely viscous liquid exhibiting a glass transition at 0 °C. Isomerization from the *N*- to the *S*-coordinated isomer occurred upon UV photoirradiation or heating, although thermal isomerization was accompanied by significant decomposition. The *N*- and *S*-coordinated isomers were separated into brown and orange liquids, respectively, using gel-permeation chromatography. Each isomer exhibited a small

solvatochromic absorption shift in organic solvents, with different solvent dependences observed for the two isomers.

INTRODUCTION

Ionic liquids, which are salts with melting points below 100 °C, exhibit versatile properties including low volatility, flame retardancy, and high ionic conductivity, with physical properties that may be tuned via component modification.¹ Therefore, extensive research on ionic liquids has been conducted in numerous fields, such as electrochemistry and organic synthesis. Ionic liquids are typically onium salts, although various functional ionic liquids containing metal complexes have been synthesized in recent years.^{2–7} Our laboratory has synthesized several ionic liquids containing cationic sandwich or half-sandwich complexes,^{8–10} which exhibit unique functionalities such as magnetism, chemical reactivity, and stimuli responsiveness in addition to ionic conductivity.^{11–14}

Linkage isomerization is a typical reaction of metal complexes with ambidentate ligands.¹⁵ *S*- and *N*-coordinated isomers exist for metal complexes bearing a thiocyanate (SCN^-) ligand, and several studies have investigated their linkage isomerizations.^{15–25} Noteworthy examples include vapor-induced solid-state isomerization, which enables colorimetric vapor detection,^{21,22} and photoisomerization associated with a spin transition.²³ Although such studies focus mainly on simple polypyridyl complexes, some half-sandwich thiocyanate compounds also exhibit linkage isomerization.^{24–26} We hypothesized that the isomerization mechanism may be useful for developing novel stimuli-responsive organometallic ionic liquids.

In this study, an ionic liquid containing a cationic half-sandwich Ru thiocyanate complex, $[\text{Ru}(\text{C}_6\text{H}_6)(\text{NCS})\text{L}]\text{Tf}_2\text{N}$ (L = *N*-hexyl-2-pyridinemethanimine, Tf_2N^- = bis(trifluoromethanesulfonyl)amide anion, $(\text{CF}_3\text{SO}_2)_2\text{N}^-$), was synthesized (**[1]** Tf_2N , **Figure 1**).

The ligand with the hexyl group and the Tf₂N anion was used to lower the melting point, and the ionic liquid was obtained as a mixture of *N*- and *S*-coordinated isomers. This paper reports the thermal properties, viscosity, and photoinduced and thermal isomerization of the synthesized ionic liquid. In addition, the solvatochromic behavior of each isomer was examined. Although photoisomerization of Ru complexes with ambidentate ligands such as NO has been well documented,²⁷⁻³⁰ there seems to be no example of the photoisomerization in Ru–SCN complexes.

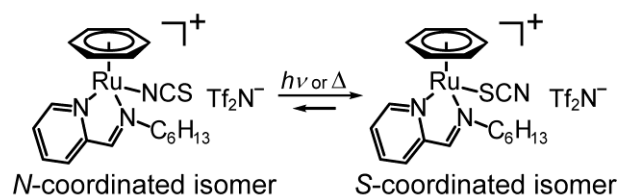


Figure 1. Linkage isomers of the half-sandwich complex [1]Tf₂N synthesized in this study.

RESULTS AND DISCUSSION

Preparation and Properties. [1]Tf₂N, obtained as a 0.7:0.3 mixture of *N*- and *S*-coordinated isomers, was an extremely viscous, sticky liquid.

The precursor [1]PF₆ was obtained as a light green powder by the reaction of [RuCl(C₆H₆)L]PF₆, AgPF₆, and KSCN at ambient temperature (81% yield). The powder was a 0.7:0.3 mixture of *N*- and *S*-coordinated isomers, as determined by ¹H NMR spectroscopy (**Figure S1**, Supporting Information). This salt was an amorphous solid at ambient temperature. [1]Tf₂N was obtained as a dark brown liquid by the reaction of [1]PF₆ with KTf₂N (86% yield). The isomer ratio was unchanged by anion exchange. The dominant *N*-coordinated isomer is the kinetic product in acetone, whereas the *S*-coordinated isomer is more thermodynamically stable, as shown below.

The isomers of [1]Tf₂N were separated using gel permeation chromatography. The droplets of the *N*- and *S*-coordinated liquids were brown and orange, respectively, whereas the liquid films

sandwiched between quartz plates appeared dark and light yellow, respectively. Photographs and UV–vis spectra of the isomers are shown in **Figure 2**. The spectrum of the *N*-coordinated isomer shows a broad peak at approximately 400 nm, whereas that of the *S*-coordinated isomer exhibits small shoulders at approximately 450 nm. The greater absorbance of the former in the visible region is consistent with its darker color. In the IR spectra, the CN stretching vibration peaks for the *N*- and *S*-coordinated isomers were observed at 2096 and 2109 cm^{-1} , respectively (**Figure S2**, Supporting Information). This is consistent with the data for the half-sandwich complex $[\text{Ru}(p\text{-cymene})(\text{bpy})(\text{SCN})]\text{PF}_6$ (bpy = 2,2'-bipyridine), with the corresponding peaks observed at 2099 and 2109 cm^{-1} , respectively.²⁶ **[1]Tf₂N** (0.7:0.3 mixture of *N*- and *S*-coordinated isomers) was mainly used for the measurements described below owing to the scarcity of the separated samples.

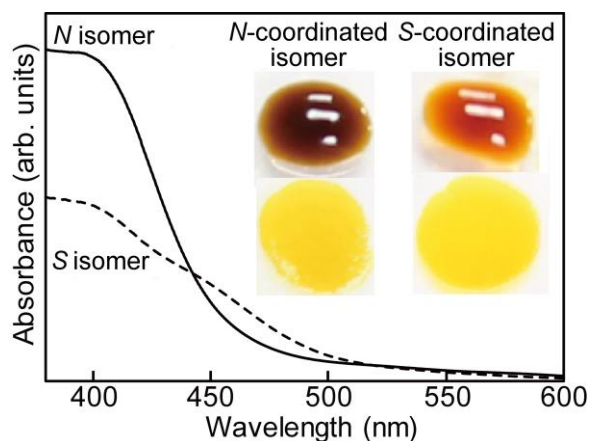


Figure 2. UV–vis spectra of the *N*-coordinated (—) and *S*-coordinated (---) isomers of **[1]Tf₂N**. Photographs of the isomers are shown in the inset: droplets on quartz plates (upper) and films sandwiched between quartz plates (lower).

Viscosity and Thermal Properties. **[1]Tf₂N** exhibited an extremely high viscosity, with a glass transition at 0 °C, and underwent thermal decomposition when heated above 125 °C.

The viscosity of [1]Tf₂N measured between 20 and 80 °C is shown in **Figure 3a** (filled circles). The liquid exhibited extremely high viscosities of 7900 and 7.6 Pa s at 25 and 80 °C, respectively, which are three to five orders of magnitude higher than those of common ionic liquids (*c.f.* [Emim]Tf₂N: 4.0×10^{-2} and 8.0×10^{-3} Pa s at 25 and 80 °C, respectively³¹). The temperature dependence of viscosity was fitted to the Vogel–Fulcher–Tammann (VFT) equation, $\eta = \eta_0 \exp(DT_0/(T - T_0))^{32}$ (**Figure 3a**), where η_0 , T_0 , and D are the viscosity at infinite temperature, the ideal glass transition temperature, and a measure of the fragility of the glass, respectively. The obtained parameters were $\eta_0 = 1.4(0.7) \times 10^{-6}$ Pa·s, $T_0 = 158(3)$ K, and $D = 22(1)$ (standard deviations in parentheses). Thermal decomposition did not occur during the measurements.

Differential scanning calorimetry (DSC) showed that [1]Tf₂N displays a glass transition at 0 °C and no crystallization at low temperatures. The high glass transition temperature was consistent with the extremely high viscosity at ambient temperature. We also performed DSC analysis of the precursor, [1]PF₆. This amorphous solid exhibited a glass transition at 60 °C, above which it became a liquid. The DSC thermograms are shown in **Figure S3** (Supporting Information).

The thermal stability of the liquid was examined using thermogravimetric–differential thermal analysis (TG-DTA). The liquid was much less thermally robust than typical onium ionic liquids. The TGA thermogram of [1]Tf₂N measured at a heating rate of 3 °C min⁻¹ is shown in **Figure 3b**. The onset of mass loss was observed at approximately 125 °C, and the temperature at which 3 wt% mass loss occurred was 162 °C. Mass loss occurred in three steps, with corresponding changes observed in the DTA thermogram. In the first step, a small mass loss (9 wt%) occurred in the range 130–200 °C, likely corresponding to the dissociation of the benzene ring (*calc.* 11 wt%). Thermal dissociation of benzene was also observed when the sample was heated in solution. The second and third mass loss steps occurred at 200–300 °C (20 wt%) and above, respectively. [1]PF₆

displayed a similar TGA thermogram (**Figure S4**, Supporting Information), indicating that the successive decomposition of the cation accounted for the mass losses observed for both salts.

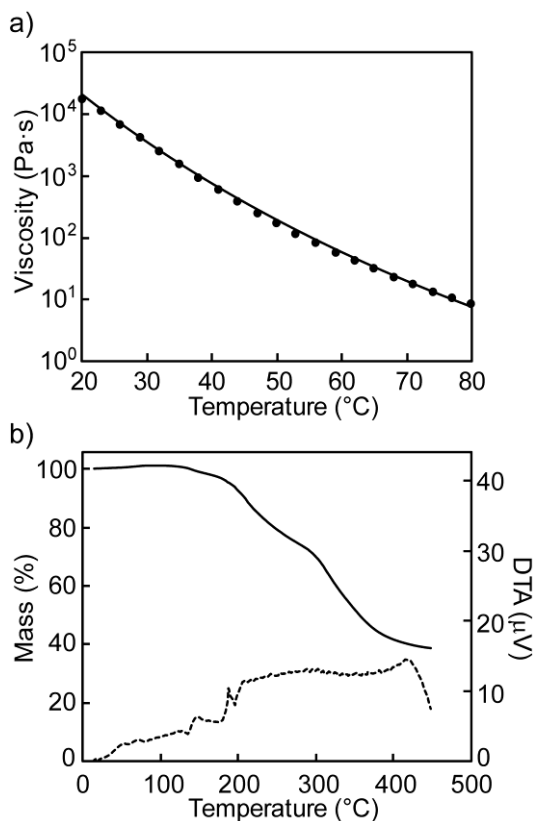


Figure 3. (a) Temperature dependence of the viscosity of [1]Tf₂N (shear rate 1 s⁻¹). The curves are fitted using the VFT equation. (b) TG (—) and DTA (---) thermograms of [1]Tf₂N (3 °C min⁻¹ under N₂).

Photoisomerization. [1]Tf₂N exhibited photoisomerization from the *N*- to the *S*-coordinated isomer, which was an equilibrium reaction.

Upon UV photoirradiation of [1]Tf₂N sandwiched between quartz plates for 90 min (365 nm, LED light), the ratio of the *N*- and *S*-coordinated isomers was changed from 7:3 to 0.45:0.55, and the amount of *S*-coordinated isomer exceeded that of the *N*-coordinated isomer. No distinct color changes were observed upon isomerization. The photoisomerization of the isolated *N*-coordinated

isomer was monitored via IR spectroscopy (**Figure S5**, Supporting Information). The spectra showed a shift in the CN stretching peak in accordance with isomerization. To examine the reversibility of photoisomerization, the photoisomerization of the isolated *S*-coordinated isomer was also investigated; after 90 min of photoirradiation, the ratio of the *N*-coordinated and *S*-coordinated isomers was changed from 0:1 to 0.24:0.76. The presence of the *N*-coordinated isomer indicates the occurrence of a reverse reaction, demonstrating that isomerization is an equilibrium reaction. Photoisomerization was accompanied by slight decomposition (4%), and the liquid became darker in color in this case. The decomposition appeared to be of thermal origin (see below), because an increase in the LED power increased the decomposition with only a slight change in the isomer ratio. To determine whether the isomerization affected the physical properties, the viscosity of [1]Tf₂N was measured before and after photoirradiation, with no changes observed.

Several Co(III) and Pt(II) thiocyanate complexes are known to exhibit photoisomerization in solution.^{20–23} The complexes typically isomerize to their kinetically stable forms in aprotic solvents.²¹ The current photoisomerization result suggests that the *S*-coordinated isomer may be kinetically favored in the ionic liquid state, although the *N*-coordinated isomer was the kinetic product in acetone. Furthermore, it was found that the photoirradiation of [1]Tf₂N in solution was ineffective for inducing isomerization; an acetonitrile coordinated complex [Ru(CH₃CN)₃(NCS)L]⁺ was formed in acetonitrile, whereas only unidentifiable products were formed in methanol and CH₂Cl₂.

Thermal Isomerization. Thermal isomerization from the *N*- to the *S*-coordinated isomer was observed in [1]Tf₂N at elevated temperatures. The isomerization direction was the same as that of photoisomerization, but the reaction was accompanied by severe decomposition.

After heating [1]Tf₂N at 80 °C for 4 h, the ratio of the *N*- and *S*-coordinated isomers was reversed from 0.7:0.3 to 0.35:0.65. This result indicates that the *S*-coordinated isomer is more thermodynamically stable than the *N*-coordinated isomer. Density functional theory (DFT) calculations revealed that the *S*-coordinated isomer is 4.2 kJ mol⁻¹ more stable than the *N*-coordinated isomer, which is consistent with the experimental result (**Figure S6**, Supporting Information). However, thermal isomerization was accompanied by severe decomposition (~50%). This decomposition occurred upon the thermal release of benzene from the cation, which yielded a decomposition product insoluble in chloroform. At higher temperatures, the ratio of the *S*-coordinated isomer was increased further, but the decomposition was increased, whereas isomerization did not occur at ambient temperature. The details thereof are provided in the experimental section. Furthermore, the thermal isomerization of the isolated *S*-coordinated isomer was examined. After 4 h of heating at 80 °C, the ratio of the *N*- and *S*-coordinated isomers changed from 0:1 to 0.13:0.87, accompanied by decomposition. This result demonstrates the occurrence of a reverse reaction, and this indicates that thermal isomerization is an equilibrium reaction.

The relative stabilities of the isomers of thiocyanate complexes depend on the complex and are also affected by the solvent.¹⁵ For [Ru(*p*-cymene)(bpy)(SCN)]⁺,²⁶ an equilibrium isomer mixture is gradually reached upon heating in solution; the *N*-coordinated isomer is favored in acetone, whereas the *S*-coordinated isomer is favored in MeOH. We examined the thermal isomerization of [1]Tf₂N in solution, but only decomposition was observed in MeOH and dimethyl sulfoxide (DMSO). In chloroform, the ratio of the *S*-coordinated isomer was increased, similar to the neat reaction, accompanied by decomposition.

Ionic liquids with thermally controllable isomerization can be used to record thermal histories. Unfortunately, the synthesized ionic liquid was not sufficiently thermally robust for this purpose.

However, this feature may be improved by molecular modification, considering the superior thermal stability of $[\text{Ru}(p\text{-cymene})(\text{bpy})(\text{SCN})]^+$.²⁶

Solvatochromic Behavior. The UV–vis spectra of the $[\mathbf{1}]\text{Tf}_2\text{N}$ isomers were measured in organic solvents. The isomers exhibited solvatochromic absorption shifts with different solvent dependences, although the shifts were slight and not visually distinguishable.

The solutions of each isomer in CH_2Cl_2 , MeCN, acetone, and MeOH were all yellow in color. The spectrum of the *N*-coordinated isomer shows a peak at approximately 400 nm (**Figure 4**), which exhibits a small solvatochromic shift (**Figure 4**, upper inset). The λ_{max} in each solvent decreased in the following order: CH_2Cl_2 (400 nm) > acetone (397 nm) > MeCN (394 nm) > MeOH (391 nm). On the other hand, the *S*-coordinated isomer exhibited a much smaller shift with a different solvent dependence. The spectrum displays a shoulder at approximately 450 nm (**Figure 4**, lower inset), which is blue-shifted in the following order: acetone (450 nm) > MeCN (448 nm) > CH_2Cl_2 (445 nm) = MeOH (445 nm).

The trend of the solvatochromic shift for the *N*-coordinated isomer was consistent with the solvent polarities E_N^T (CH_2Cl_2 : 0.31, acetone: 0.35, MeCN: 0.46, MeOH: 0.76).³³ TD-DFT calculations predicted a UV–vis transition at 399 nm, from HOMO-1 (mixed Ru-SCN orbital) to LUMO (Ru-L orbital). This charge-transfer character accounts for the observed solvent dependence.^{34–37} In contrast, the trend of the *S*-coordinated isomer was consistent with the acceptor number AN (acetone: 12.5, MeCN: 18.9, CH_2Cl_2 : 20.4, MeOH: 41.5),³⁸ which reflects the hydrogen bonding abilities of the solvents. The correlation with AN has also been reported for the solvatochromism of Ru-pyridyl complexes with cyanide ligands.³⁹ This correlation is reasonable because the terminal N of the SCN^- ligand can form hydrogen bonds with the solvent. TD-DFT

calculations predicted low-energy transitions (HOMO to LUMO+1) at 457 and 454 nm for the *S*-bonded isomer and its hydrogen-bonded MeOH adduct, respectively, which was consistent with the observed trend.

Several Ru-SCN complexes exhibit solvatochromic behaviors,^{34–37} although no such comparative studies on their linkage isomers have been reported. Although the observed solvatochromic differences were very small, the mechanisms underlying them may be useful for controlling the solvatochromic and vapochromic behaviors of ionic liquids.

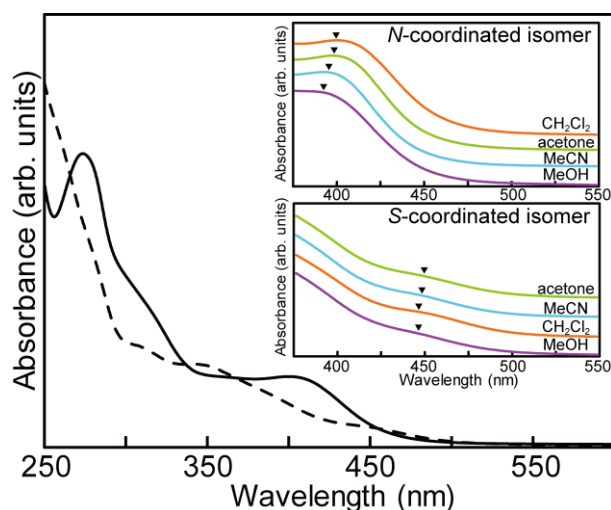


Figure 4. UV-vis spectra of the *N*-coordinated (—) and *S*-coordinated (---) isomers in CH₂Cl₂ (80 μmol L⁻¹). Their spectra in CH₂Cl₂ (orange), acetone (green), MeCN (pale blue), and MeOH (purple) are shown in the inset. The triangles indicate the peak positions derived from the fourth-order derivatives of the spectra.

CONCLUSION

An ionic liquid containing a half-sandwich Ru complex bearing a thiocyanate ligand was synthesized, yielding a mixture of *N*- and *S*-coordinated isomers in a 7:3 ratio. Photoinduced and

thermal isomerization from the *N*- to the *S*-coordinated isomer was observed, but heating was accompanied by significant decomposition. The isomers exhibited different solvatochromic absorption shifts in organic solvents. Although the solvatochromic shifts were small in the current complex, the underlying mechanism thereof may be useful for controlling the chromic behavior of ionic liquids via external stimuli.

EXPERIMENTAL SECTION

General. $[\text{Ru}(\text{C}_6\text{H}_6)\text{Cl}_2]_2$ and *N*-hexyl-2-pyridinemethanimine (L) were prepared according to literature procedures.^{40,41} Other reagents were purchased from Tokyo Chemical Industry. Preparative gel permeation liquid chromatography was performed using an LC-908 (Japan Analytical Industry Co., Ltd.) equipped with JAIGEL 1H and 2H columns (eluent: CH_2Cl_2 , flow rate: 10 mL min^{-1}). ^1H and ^{19}F NMR spectra were recorded using an Avance 400 spectrometer (Bruker). FT-IR spectra were measured using a Nicolet iS5 FT-IR spectrometer (Thermo Fisher Scientific) equipped with an attenuated total reflectance (ATR) unit (diamond). Electrospray ionization-mass spectrometry was conducted using an LTQ Orbitrap Discovery (Thermo Fisher Scientific). DSC was performed using a Q100 differential scanning calorimeter (TA Instruments) at a ramp rate of $10 \text{ }^\circ\text{C min}^{-1}$ in an aluminum hermetic pan. UV-vis spectroscopy was performed using a V-570 UV-VIS/NIR spectrophotometer (JASCO, Inc.). The samples were placed on quartz plates for the measurements. TG-DTA was performed using a TG8120 thermal analyzer (Rigaku) at a scan rate of 3 or $10 \text{ }^\circ\text{C min}^{-1}$ under a N_2 atmosphere. The viscosity was measured using a Discovery HR-2 instrument (TA Instruments). TD-DFT calculations were performed using Spartan'20 software (Wavefunction, Inc.) at the $\omega\text{B97-D/LanL2DZ}$ level.

Synthesis of [RuCl(C₆H₆)L]PF₆. Under an N₂ atmosphere, a solution of [Ru(C₆H₆)Cl₂]₂ (250 mg, 0.50 mmol) and L (194 mg, 1.02 mmol) in MeOH (10 mL) was stirred at ambient temperature for 2 h, as the color of the solution changed from red to dark brown. NH₄PF₆ (371 mg, 2.28 mmol) was then added to the solution, and stirring was continued for 1 h. The precipitated yellow powder was collected by vacuum filtration. The addition of diethyl ether to the filtrate and subsequent cooling to -4 °C yielded an additional batch, which was collected by filtration and dried under vacuum (499 mg, 91% yield). ¹H NMR (400 MHz, CDCl₃): δ = 0.90 (t, 3H, CH₃, *J* = 6.94 Hz), 1.31–1.44 (br, 6H, CH₂), 1.96–2.03 (br, 2H, CH₂), 4.33 (quin, 1H, CH₂, *J* = 7.37 Hz), 4.48 (quin, 1H, CH₂, *J* = 7.12 Hz), 5.97 (s, 6H, arene), 7.61 (s, 1H, CH, *J* = 7.30 Hz), 7.91 (d, 1H, CH, *J* = 7.76 Hz), 8.04 (t, 1H, CH, *J* = 7.74 Hz), 8.25 (s, 1H, CH), 9.22 (d, 1H, CH, *J* = 5.56 Hz). FT-IR (ATR, cm⁻¹): 556 (P–F), 770, 829 (P–F), 1163, 1240, 1306, 1438, 1480, 1597, 2359, 2858, 2939, 3081. ESI-MS: *m/z* calcd. for C₁₈H₂₄ClN₂Ru⁺: 405.0666. Found: 405.0660.

Synthesis of [Ru(C₆H₆)(NCS)L]PF₆ ([1]PF₆). AgPF₆ (208 mg, 0.82 mmol) was added to an acetone solution (6 mL) of [RuCl(C₆H₆)L]PF₆ (298 mg, 0.54 mmol), and the mixture was stirred at ambient temperature for 60 h. AgCl was then removed by filtration. The complete reaction of [RuCl(C₆H₆)L]PF₆ was confirmed by ¹H NMR spectroscopy. KSCN (269 mg, 2.77 mmol) was subsequently added to the filtrate, and the mixture was stirred for 3 h. After solvent evaporation, the residue was dissolved in CH₂Cl₂ (15 mL), an aqueous solution (15 mL) of NH₄PF₆ (236 mg, 1.45 mmol) was added, and the resulting mixture was stirred vigorously. The organic layer was separated, washed twice with water (15 mL), and dried over anhydrous MgSO₄. After solvent removal, diethyl ether was added to the remaining powder and the dispersion was sonicated to remove ether-soluble impurities. The product was collected by filtration as a light green powder

(250 mg, yield 81%). The product was a mixture of *N*- and *S*-coordinated isomers in a 0.7:0.3 ratio. ^1H NMR (400 MHz, CDCl_3) for *N*-bound isomer: δ = 0.93 (m, 3H, CH_3), 1.35–1.40 (br, 6H, CH_2), 2.28–2.37 (m, 2H, CH_2), 4.24–4.31 (br, 2H, CH_2), 6.04 (s, 6H, arene), 7.68 (m, 1H, CH), 7.95–8.16 (m, 2H, CH), 8.36 (s, 1H, CH), 9.07 (d, 1H, CH , J = 10.16 Hz). *S*-bound isomer: δ = 0.93 (m, 3H, CH_3), 1.35–1.40 (br, 6H, CH_2), 2.28–2.37 (m, 2H, CH_2), 4.24–4.31 (br, 2H, CH_2), 6.02 (s, 6H, arene), 7.68 (m, 1H, CH), 7.95–8.16 (m, 2H, CH), 8.31 (s, 1H, CH), 9.16 (d, 1H, CH , J = 10.16 Hz). ESI-MS: m/z calcd. for $\text{C}_{19}\text{H}_{24}\text{N}_3\text{RuS}^+$: 428.0734. Found: 428.0747. Anal. Calcd. for $\text{C}_{19}\text{H}_{24}\text{F}_6\text{N}_3\text{PRuS}$: C, 39.79; H, 4.22; N, 7.33. Found: C, 39.90; H, 4.27; N, 7.22.

Synthesis of $[\text{Ru}(\text{C}_6\text{H}_6)(\text{NCS})\text{L}]\text{Tf}_2\text{N}$ ($[\mathbf{1}]\text{Tf}_2\text{N}$). An aqueous solution (5 mL) of KTf_2N (316 mg, 0.99 mmol) was added to a CH_2Cl_2 solution (5 mL) of $[\mathbf{1}]\text{PF}_6$ (183 mg, 0.33 mmol), and the mixture was stirred vigorously for 30 min at ambient temperature. The organic layer was collected, and the anion-exchange procedure was repeated thrice. The organic layer was dried over anhydrous MgSO_4 and filtered, before the solvent was removed using a rotary evaporator. The absence of PF_6^- was confirmed by ^{19}F NMR spectroscopy. The product was dried under vacuum at 40 °C overnight, yielding the desired dark brown liquid (203 mg, 86% yield). This liquid was a mixture of *N*- and *S*-coordinated isomers in a 0.7:0.3 ratio. Small quantities of the *N*- and *S*-coordinated isomers were separated using gel permeation chromatography (eluent: chloroform, flow rate 10 mL min^{-1}). The retention times were 20.8 and 20.4 min, respectively. ^1H NMR (400 MHz, DMSO) *N*-bound isomer: δ = 0.88 (m, 3H, CH_3), 1.34 (s, 6H, CH_2), 1.75–1.80 (m, 1H, CH_2), 1.93–1.97 (m, 1H, CH_2), 4.19–4.26 (m, 1H, CH_2), 4.58–4.64 (m, 1H, CH_2), 6.24 (s, 6H, arene), 7.89 (m, 1H, CH), 8.24 (t, 1H, CH , J = 6.98 Hz), 8.33 (t, 1H, CH , J = 8.36 Hz), 8.87 (s, 1H, CH), 9.62 (d, 1H, CH , J = 5.28 Hz). *S*-bound isomer: δ = 0.88 (m, 3H, CH_3), 1.34 (s, 6H, CH_2), 1.75–1.80 (m, 1H, CH_2),

1.93–21.97 (m, 1H, CH_2), 4.28–4.34 (m, 1H, CH_2), 4.38–4.45 (m, 1H, CH_2), 6.23 (s, 6H, arene), 7.81 (m, 1H, CH), 8.24 (t, 1H, CH , $J = 6.98$ Hz), 8.33 (t, 1H, CH , $J = 8.36$ Hz), 8.89 (s, 1H, CH), 9.43 (d, 1H, CH , $J = 5.52$ Hz). FT-IR (ATR, cm^{-1}): 528, 739, 770, 788, 839, 1226, 1347, 1439, 1480, 1599, 2099 (CN), 2859, 2931, 3085. ESI-MS: m/z calcd. for $\text{C}_{19}\text{H}_{24}\text{N}_3\text{RuS}^+$: 428.0734. Found: 428.0746. Anal. Calcd. for $\text{C}_{19}\text{H}_{24}\text{F}_6\text{N}_3\text{PRuS}$: C, 35.61; H, 3.42; N, 7.91. Found: C, 36.17; H, 3.45; N, 7.62.

Photoinduced and thermal isomerizations of [1]Tf₂N. Photoisomerization was performed with the samples sandwiched between quartz plates using an LC-L1V3 Lightningcure UV-LED lamp (365 nm, 180 mW cm^{-2} , Hamamatsu Photonics) as the light source. The sample was placed on a cooling plate set at 10 °C during photoirradiation. Upon photoirradiation, the *N*-isomer:*S*-isomer ratio of [1]Tf₂N was changed from 0.7:0.3 to 0.45:0.55 over 90 min. In the ¹H NMR spectrum of the product, free benzene (4%) was observed at 7.3 ppm; this was released through decomposition. Photoirradiation with more intense light increased the decomposition, indicating that the generated heat caused decomposition. The reaction rates also depended on the sample thickness, because each isomer showed absorption at 365 nm. In addition, photoirradiation of the solutions of [1]Tf₂N in dichloromethane-*d*₂, chloroform-*d*₃, acetonitrile-*d*₃, and methanol-*d*₄ was performed. The product in acetonitrile-*d*₃ was identified as $[\text{Ru}(\text{CD}_3\text{CN})_3(\text{SCN})\text{L}]^+$ from the ¹H NMR and HRMS spectra, whereas the other solvents yielded only unidentifiable products.

The thermal isomerization was examined as follows. Under a N₂ atmosphere, [1]Tf₂N (19 mg, 0.026 mmol) was heated at 80 °C for 4 h. After cooling to ambient temperature, the sample was dissolved in chloroform (10 mL), and the insoluble decomposition product was removed by filtration. The solvent was removed from the filtrate under reduced pressure, and the residue was

dried under vacuum at 40 °C for 4 h (31 mg, 46% yield). The *N*-isomer:*S*-isomer ratio in the resultant liquid was 0.35:0.65. [1]Tf₂N isomerization was slower at 70 °C (isomer ratio: 0.43:0.57 at 4 h), although the yield did not improve. Isomerization was faster at 90 °C (isomer ratio: 0.28:0.72 at 4 h), but further decomposition resulted in a very low yield (6%).

The thermal isomerization of [1]Tf₂N in chloroform-*d* at 50 °C was monitored using ¹H NMR spectroscopy (**Figure S7**, Supporting Information). The ratio of the *S*-coordinated isomer increased with time, and the *N*-isomer:*S*-isomer ratio was changed from 0.7:0.3 to 0.56:0.44 over 6 days. The solution remained yellow, but a small amount of dark brown precipitate gradually formed. In the ¹H NMR spectra, signals representing free benzene gradually appeared, with ratios of 3% and 9% after 1 and 6 days, respectively, relative to the complex. The benzene ligand is released from the complex, yielding the decomposition product. In addition, reactions in other solvents were investigated. [1]Tf₂N decomposed within a few days in coordinating solvents such as DMSO-*d*₆ and methanol-*d*₄ upon heating at 50 °C, yielding numerous unidentifiable signals in the ¹H NMR spectra.

AUTHOR INFORMATION

Corresponding Author

Tomoyuki Mochida, Department of Chemistry, Graduate School of Science and Center for Membrane Technology, Kobe University, Kobe, Hyogo 657-8501, Japan; orcid.org/0000-0002-3446-2145; Phone: +81-78-803-5679; Email: tmochida@platinum.kobe-u.ac.jp

Author

Syou Maekawa – Department of Chemistry, Graduate School of Science, Kobe University, Kobe,

Hyogo 657-8501, Japan

Ryo Sumitani, Department of Chemistry, Graduate School of Science, Kobe University, Kobe,
Hyogo 657-8501, Japan; orcid.org/0000-0002-6617-2994

Complete contact information is available at: <https://pubs.acs.org/>

Notes

The author declare no competing financial interest.

ACKNOWLEDGMENTS

This work was financially supported by KAKENHI (grant number 20H02756) from the Japan Society for the Promotion of Science (JSPS) and a Grant-in-Aid for JSPS Research Fellows (grant number 21J12056).

Supporting Information

The supporting Information is available free of charge at <http://pubs.acs.org>.

¹H NMR, IR, and UV-vis spectral data, DSC and TG-DTA thermograms, and DFT calculation results (PDF)

REFERENCES

(1) Kar, M.; Matuszek, K.; MacFarlane, D. R. Ionic Liquids, In *Kirk–Othmer Encyclopedia of Chemical Technology*; John Wiley & Sons, Inc., **2019**, DOI: 10.1002/0471238961.ionisedd.a01.pub2.

- (2) Brooks, N. R.; Schaltin, S.; Van Hecke, K.; Van Meervelt, L.; Binnemans, K.; Fransaer, J. Copper(I)-Containing Ionic Liquids for High-Rate Electrodeposition. *Chem. - Eur. J.* **2011**, *17*, 5054–5059.
- (3) Branco, A.; Branco, L. C.; Pina, F. Electrochromic and Magnetic Ionic Liquids. *Chem. Commun.* **2011**, *47*, 2300–2302.
- (4) Zhang, P.; Gong, Y.; Lv, Y.; Guo, Y.; Wang, Y.; Wang, C.; Li, H. Ionic Liquids with Metal Chelate Anions. *Chem. Commun.* **2012**, *48*, 2334–2336.
- (5) Osborne, S. J.; Wellens, S.; Ward, C.; Felton, S.; Bowman, R. M.; Binnemans, K.; Swadźba-Kwaśny, M.; Gunaratne, H. Q. N.; Nockemann, P. Thermochromism and Switchable Paramagnetism of Cobalt(II) in Thiocyanate Ionic Liquids. *Dalton Trans.* **2015**, *44*, 11286–11289.
- (6) Billeci, F.; Gunaratne, H. Q. N.; Licence, P.; Seddon, K. R.; Plechkova, N. V.; D’Anna, F. Ionic Liquids–Cobalt(II) Thermochromic Complexes: How the Structure Tunability Affects “Self-Contained” Systems. *ACS Sustainable Chem. Eng.* **2021**, *9*, 4064–4075.
- (7) Ma, L.; Haynes, C. J. E.; Grommet, A. B.; Walczak, A.; Parkins, C. C.; Doherty, C. M.; Longley, L.; Tron, A.; Stefankiewicz, A. R.; Bennett, T. D.; Nitschke, J. R. Coordination Cages as Permanently Porous Ionic Liquids. *Nat. Chem.* **2020**, *12*, 270–275.
- (8) Inagaki, T.; Mochida, T.; Takahashi, M.; Kanadani, C.; Saito, T.; Kuwahara, D. Ionic Liquids of Cationic Sandwich Complexes. *Chem. - Eur. J.* **2012**, *18*, 6795–6804.
- (9) Inagaki, T.; Abe, K.; Takahashi, K.; Mochida, T. Organometallic Ionic Liquids from Half-Sandwich Ru(II) Complexes with Various Chelating Ligands. *Inorg. Chim. Acta* **2015**, *438*, 112–117.
- (10) Inagaki, T.; Mochida, T. Reactive Half-Metallocenium Ionic Liquids That Undergo Solventless Ligand Exchange. *Chem. - Eur. J.* **2012**, *18*, 8070–8075.

- (11) Funasako, Y.; Mochida, T.; Inagaki, T.; Sakurai, T.; Ohta, H.; Furukawa, K.; Nakamura, T. Magnetic Memory Based on Magnetic Alignment of a Paramagnetic Ionic Liquid Near Room Temperature. *Chem. Commun.* **2011**, 47, 4475–4477.
- (12) Funasako, Y.; Mori, S.; Mochida, T. Reversible Transformation between Ionic Liquids and Coordination Polymers by Application of Light and Heat. *Chem. Commun.* **2016**, 52, 6277–6279.
- (13) Ueda, T.; Tominaga, T.; Mochida, T.; Takahashi, K.; Kimura, S. Photogeneration of Microporous Amorphous Coordination Polymers from Organometallic Ionic Liquids. *Chem. –Eur. J.* **2018**, 24, 9490–9493.
- (14) Sumitani, R.; Yoshikawa, H.; Mochida, T. Reversible Control of Ionic Conductivity and Viscoelasticity of Organometallic Ionic Liquids by Application of Light and Heat. *Chem. Commun.* **2020**, 56, 6189–6192.
- (15) Burmeister, J. Ambidentate Ligands, the Schizophrenics of Coordination Chemistry. *Coord. Chem. Rev.* **1990**, 105, 77–133.
- (16) Nazeeruddin, M. K.; Grätzel, M. Separation of Linkage Isomers of Trithiocyanato (4,4',4''-tricarboxy-2,2',6,2''-terpyridine)ruthenium(II) by pH-titration Method and their Application in Nanocrystalline TiO₂-based Solar Cells. *J. Photochem. Photobiol., A* **2001**, 145, 79–86.
- (17) Kakoti, M.; Chaudhury, S.; Deb, A. K.; Goswami, S. Isomeric Dithiocyanate Complexes of Ruthenium(II), Synthesis, Characterization of all Possible Bond Isomers of *trans,cis*-Ru(CNS)₂L₂ [L = 2-(aryloxy)pyridine] and Studies of Isomerization. *Polyhedron* **1993**, 12, 783–789.
- (18) Brewster, T. P.; Ding, W.; Schley, N. D.; Hazari, N.; Batista, V. S.; Crabtree, R. H. Thiocyanate Linkage Isomerism in a Ruthenium Polypyridyl Complex. *Inorg. Chem.* **2011**, 50, 11938–11946.
- (19) Saxena, P.; Thomas, J. M.; Sivasankar, C.; Thirupathi, N. Syntheses and Structural Aspects

of Six-membered Palladacyclic Complexes Derived from *N,N',N''*-Triarylguanidines with N- or S-Thiocyanate Ligands. *New J. Chem.* **2019**, *43*, 2307–2327.

(20) Melpolder, J. B.; Burmeister, J. L. Solvent and Counteraction Effects on Ambidentate Bonding Patterns in Thiocyanato- and Selenocyanatopentacyanocobaltate(III) Complexes. *Inorg. Chim. Acta* **1975**, *15*, 91–104.

(21) Kishi, S.; Kato, M. Thermal and Photo Control of the Linkage Isomerism of Bis(thiocyanato)(2,2'-bipyridine)platinum(II), *Inorg. Chem.* **2003**, *42*, 8728–8734.

(22) Kobayashi, A.; Fukuzawa, Y.; Chang, H.-C.; Kato, M. Vapor-Controlled Linkage Isomerization of a Vapochromic Bis(thiocyanato)platinum(II) Complex: New External Stimuli To Control Isomerization Behavior. *Inorg. Chem.* **2012**, *51*, 7508–7519.

(23) Sheu, C.-F.; Shih, C.-H.; Sugimoto, K.; Cheng, B.-M.; Takata, M.; Wang, Y. A Long-lived Photo-induced Metastable State of Linkage Isomerization Accompanied with a Spin Transition. *Chem. Commun.* **2012**, *48*, 5715–5717.

(24) Sloan, T. E.; Wojcicki, A. Linkage Isomerism in Carbonyl- π -cyclopentadienyl(thiocyanato)metal Complexes. *Inorg. Chem.* **1968**, *7*, 1268–1273.

(25) Wang, F.; Habtemariam, A.; van der Geer, E. P. L.; Deeth, R. J.; Gould, R.; Parsons, S.; Sadler, P. J. *J. Biol. Inorg. Chem.* **2009**, *14*, 1065–1076.

(26) Vandenburg, L.; Buck, M. R.; Freedman, D. A. Preparation, Separation, and Characterization of Ruthenium(II) Thiocyanate Linkage Isomers. *Inorg. Chem.* **2008**, *47*, 9134–9136.

(27) Mikhailov, A. A.; Stolyarova, E. D.; Kostin, G.A. Photochemistry of Ruthenium Nitrosyl Complexes in Solids and Solutions and its Potential Applications. *J. Struct. Chem.* *62*, 497–516 (2021).

(28) Coppens, P.; Novozhilova, I; Kovalevsky, A. Photoinduced Linkage Isomers of Transition-

- Metal Nitrosyl Compounds and Related Complexes. *Chem. Rev.* **2002**, *102*, 861–884.
- (29) Kovalevsky, A. Y.; Bagley, K. A.; Cole, J. M.; Coppens, P. Light-induced Metastable Linkage Isomers of Ruthenium Sulfur Dioxide Complexes. *Inorg. Chem.* **2003**, *42*, 140–147.
- (30) Butcher, D. P.; Rachford, A. A.; Petersen, J. L.; Rack, J. J. Phototriggered S → O Isomerization of a Ruthenium-Bound Chelating Sulfoxide. *Inorg. Chem.* **2006**, *45*, 9178–9180.
- (31) Makino, T.; Kanakubo, M.; Masuda, Y.; Umecky, T.; Suzuki, A. CO₂ Absorption Properties, Densities, Viscosities, and Electrical Conductivities of Ethylimidazolium and 1-Ethyl-3-methylimidazolium Ionic Liquids. *Fluid Phase Equilib.* **2014**, *362*, 300–306.
- (32) Fulcher, G. S. Analysis of Recent Measurements of the Viscosity of Glasses. *J. Am. Ceram. Soc.* **1925**, *8*, 339–355.
- (33) Reichardt, C. Solvatochromic Dyes as Solvent Polarity Indicators. *Chem. Rev.* **1994**, *94*, 2319–2358.
- (34) Li, M.-X.; Zhou, X.; Xia, B.-H.; Zhang, H.-X.; Pan, Q.-J.; Liu, T.; Fu, H.-G.; Sun, C.-C. Theoretical Studies on Structures and Spectroscopic Properties of Photoelectrochemical Cell Ruthenium Sensitizers, [Ru(H_mtcterpy)(NCS)₃]ⁿ⁻ (*m* = 0, 1, 2, and 3; *n* = 4, 3, 2, and 1). *Inorg. Chem.* **2008**, *47*, 2312–2324.
- (35) Fantacci, S.; De Angelis, F.; Selloni, A. Absorption Spectrum and Solvatochromism of the [Ru(4,4'-COOH-2,2'-bpy)₂(NCS)₂] Molecular Dye by Time Dependent Density Functional Theory. *J. Am. Chem. Soc.* **2003**, *125*, 4381–4387.
- (36) Hu, Y.; Sanchez-Molina, I.; Haque, S. A.; Robertson, N. Ruthenium Dyes with Azo Ligands: Light Harvesting, Excited-State Properties and Relevance to Dye-Sensitised Solar Cells. *Eur. J. Inorg. Chem.* **2015**, 5864–5873.
- (37) Zhang, H.-X.; Ke, W.-S.; Zhu, C.-Y.; Wang, J.-Y.; Sasaki, Y.; Chen, Z.-N.; Lin, C.; Wang,

Z.; Liao, S.; Wu, W. Synthesis, Characterization and Properties of Oxo-bridged Diruthenium(III) Complexes with Thiocyanato and Cyanato Ligands. *Inorg. Chim. Acta* **2018**, 469, 469–477.

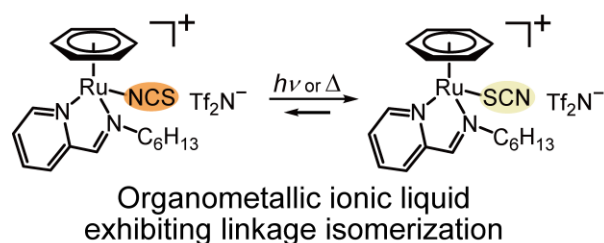
(38) Gutmann, V.; Resch, G.; Linert, W. Structural Variability in Solutions. *Coord. Chem. Rev.* **1982**, 43, 133–164.

(39) Timpson, C. J.; Bignozzi, C. A.; Sullivan, B. P.; Kober, E. M.; Meyer, T. J. Influence of Solvent on the Spectroscopic Properties of Cyano Complexes of Ruthenium(II). *J. Phys. Chem.* **1996**, 100, 2915–2925.

(40) Bennett, M. A.; Smith, A. K. Arene Ruthenium(II) Complexes Formed by Dehydrogenation of Cyclohexadienes with Ruthenium(III) Trichloride. *J. Chem. Soc., Dalton Trans.* **1974**, 233–241.

(41) Srivastava, P. K.; Choudhary, V. *N*-(*n*-Alkyl)-2-pyridinemethanimine Mediated Atom Transfer Radical Polymerization of Lauryl Methacrylate: Effect of Length of Alkyl Group. *J. Appl. Polym. Sci.* **2012**, 125, 31–37.

Table of Contents



An ionic liquid containing a cationic half-sandwich Ru thiocyanate complex was synthesized. Isomerization from the *N*- to the *S*-coordinated isomer occurred upon UV photoirradiation or heating.

Supporting Information

Photoinduced and Thermal Linkage Isomerizations of an Organometallic Ionic Liquid Containing a Half-Sandwich Ruthenium Thiocyanate Complex

Tomoyuki Mochida,^{*a,b} Syou Maekawa,^a and Ryo Sumitani^a

^a*Department of Chemistry, Graduate School of Science, Kobe University, Rokkodai, Nada, Kobe, Hyogo 657-8501, Japan. E-mail: tmochida@platinum.kobe-u.ac.jp*

^b*Research Center for Membrane and Film Technology, Kobe University, Rokkodai, Nada, Kobe, Hyogo 657-8501, Japan*

Contents

Figure S1. ¹H NMR spectra of the compounds synthesized in this study.

Figure S2. IR spectra of the *N*-coordinated and *S*-coordinated isomers and [1]Tf₂N.

Figure S3. DSC thermograms of [1]Tf₂N and [1]PF₆.

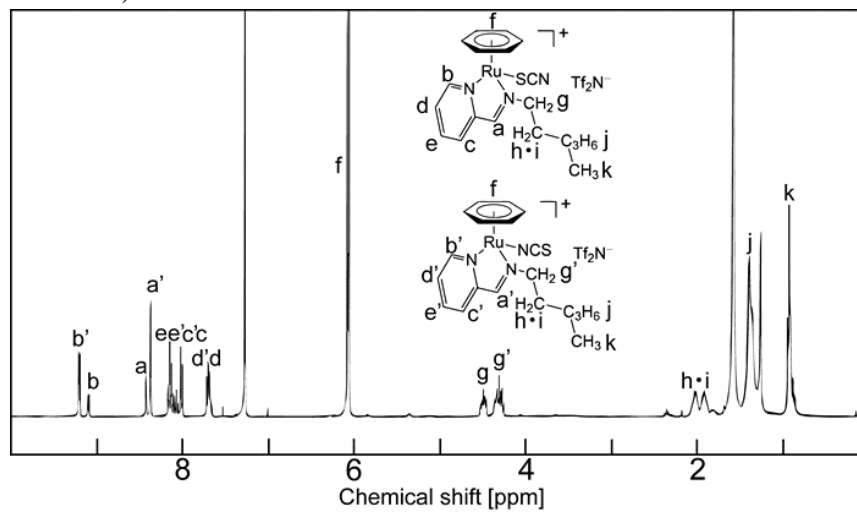
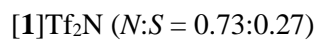
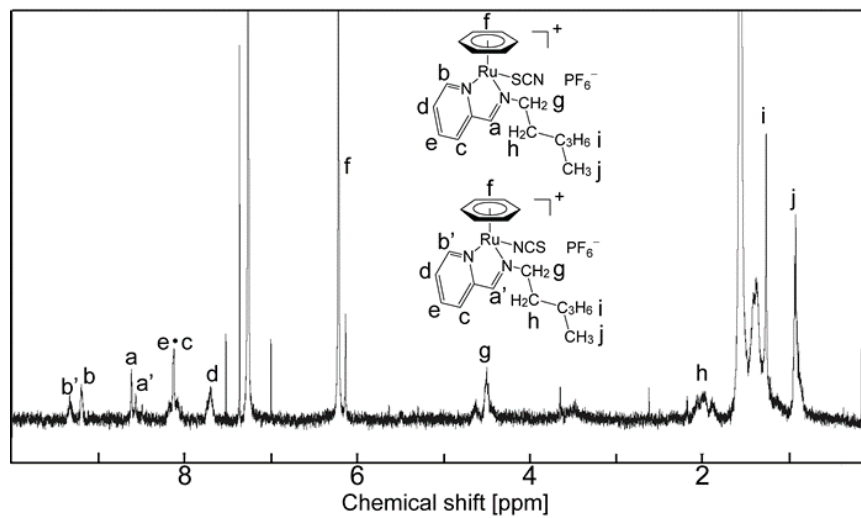
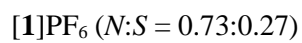
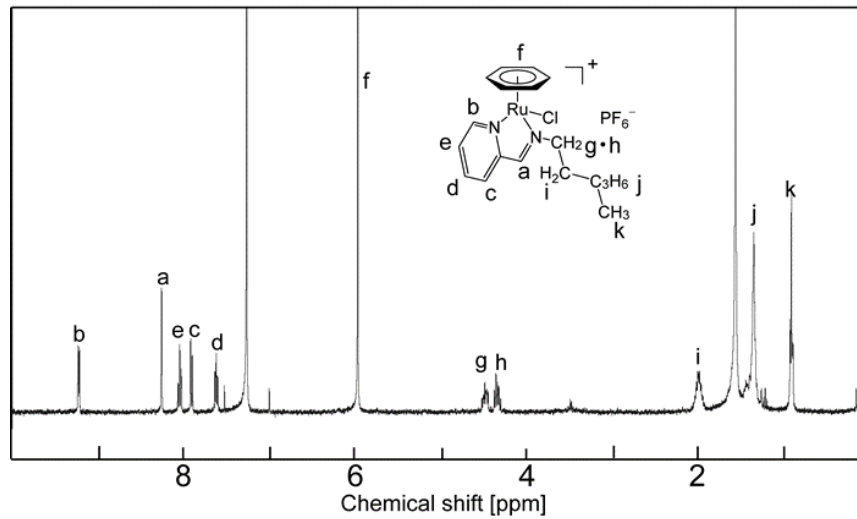
Figure S4. TG-DTA thermograms of [1]Tf₂N and [1]PF₆.

Figure S5. IR spectra of the *N*-coordinated isomer taken upon photoirradiation.

Figure S6. Optimized geometries of the *N*- and *S*-coordinated isomers obtained using DFT calculations.

Figure S7. ¹H NMR spectra of [1]Tf₂N (*N*:*S* = 0.73:0.27, CDCl₃ solution) measured before and after heating.

Figure S8. UV-Vis spectra and photographs of the *N*-coordinated and *S*-coordinated isomers in dichloromethane and methanol.



[1']Tf₂N (after thermal isomerization, *N*:*S* = 0.35:0.65)

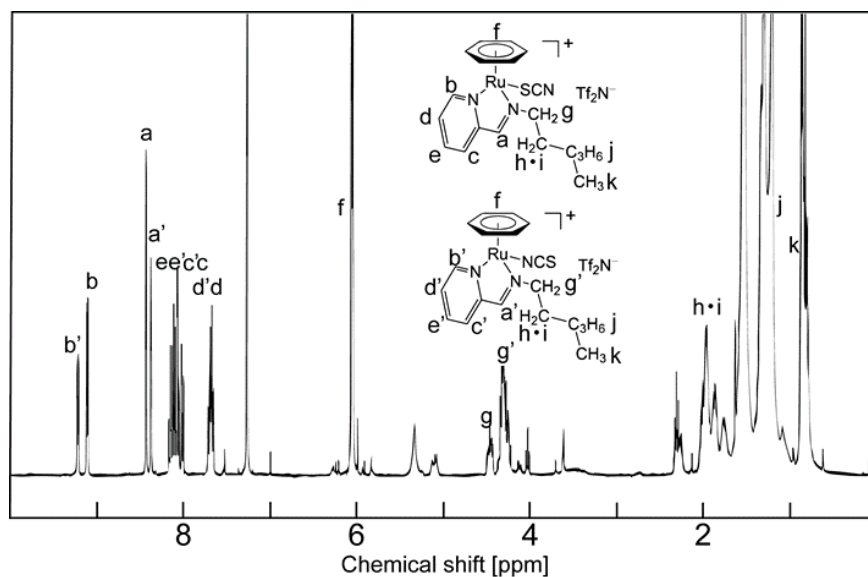


Figure S1. ¹H NMR spectra of the compounds synthesized in this study (CDCl₃).

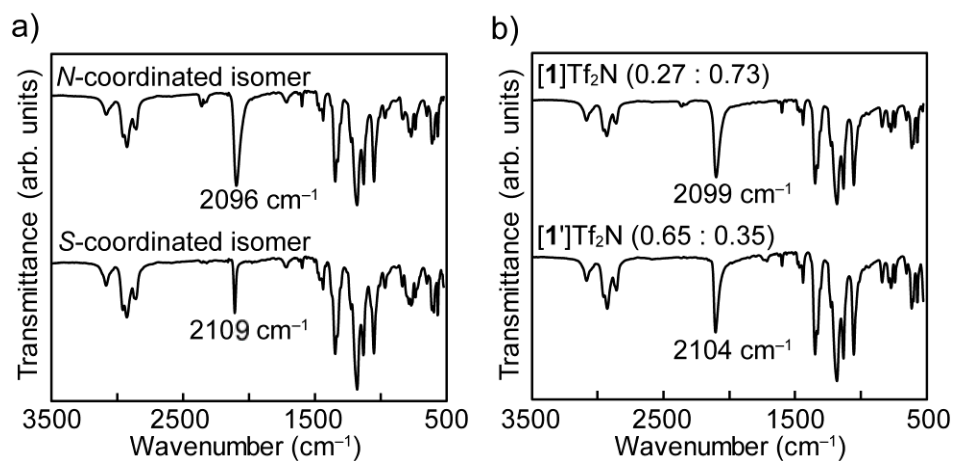


Figure S2. IR spectra of (a) the *N*-coordinated and *S*-coordinated isomers and (b) [1]Tf₂N and [1']Tf₂N (after thermal isomerization).

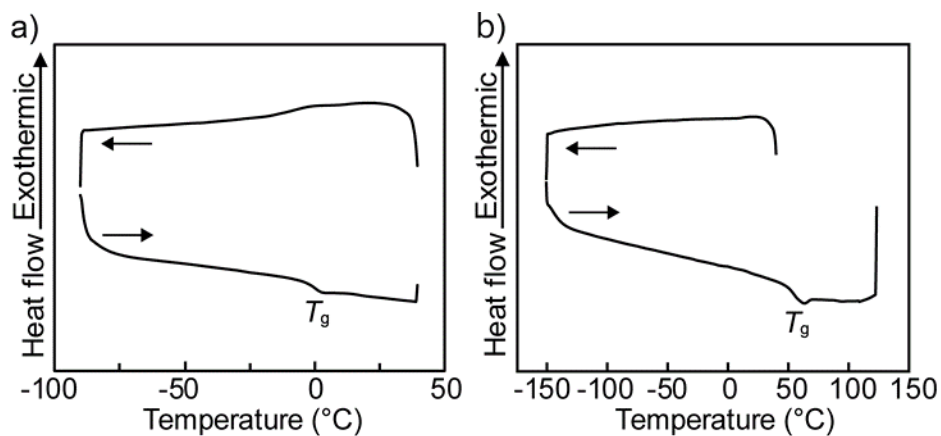


Figure S3. DSC thermograms of [1]Tf₂N (left) and [1]PF₆ (right).

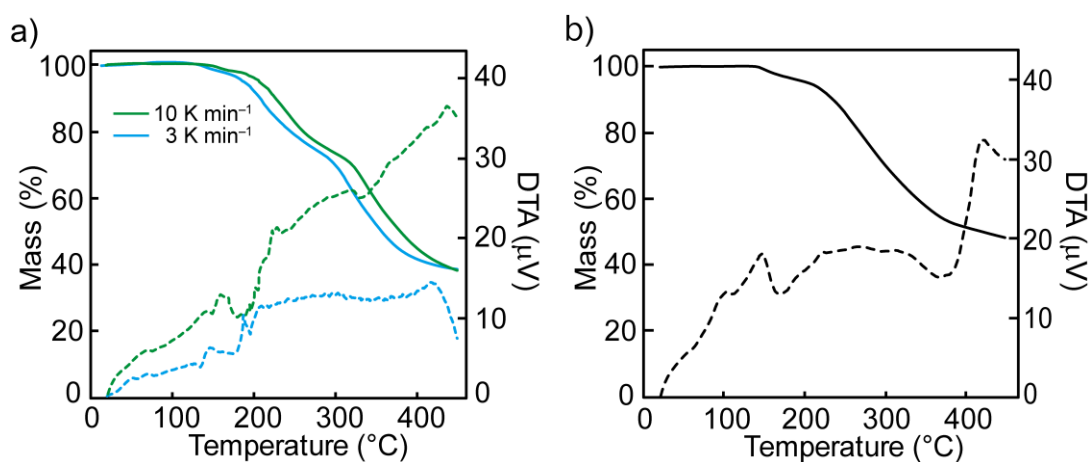


Figure S4. TG (—) and DTA (---) thermograms of (a) [1]Tf₂N (10 and 3 °C min⁻¹) and (b) [1]PF₆ (10 °C min⁻¹).

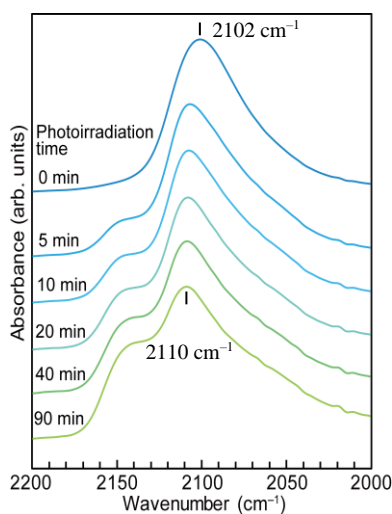


Figure S5. IR spectra of the *N*-coordinated isomer taken upon photoirradiation (KBr plate, transmission spectra).

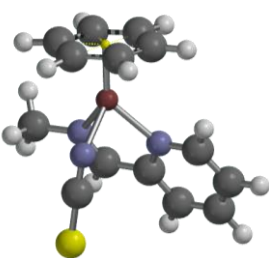
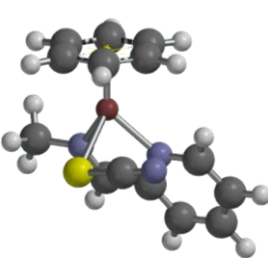
		
	<i>N</i> -coordinated isomer	<i>S</i> -coordinated isomer
$E_{\text{el+ZPE}}, G^0$ (au)	-1197.5804, -1197.6220	-1197.5820, -1197.6236
HOMO, LUMO (eV)	-10.48, -4.14	-11.10, -4.20

Figure S6. Optimized geometries of the *N*- and *S*-coordinated isomers obtained using DFT calculations. The total energy ($E_{\text{electronic+ZPE}}$), Gibbs energy (G^0), and energies of the HOMO/LUMO levels of each isomer are shown below each structure.

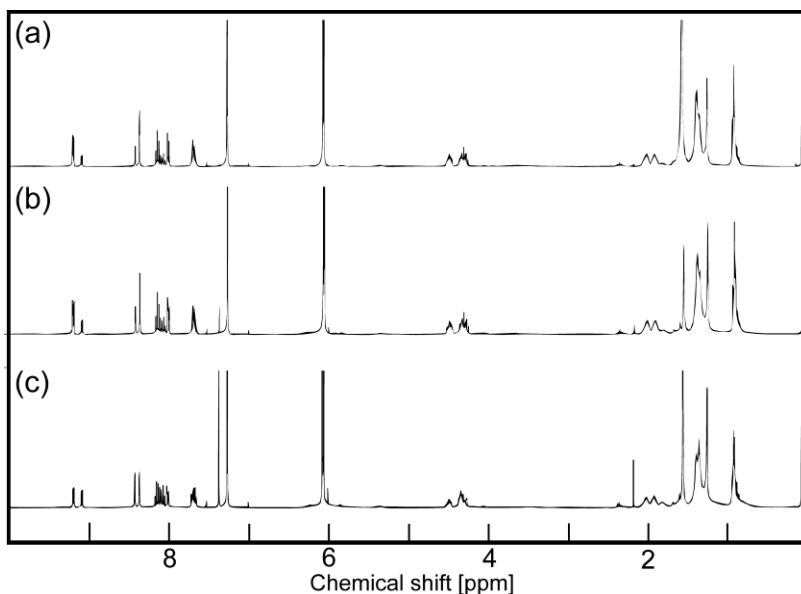


Figure S7. ^1H NMR spectra of $[\mathbf{1}]\text{Tf}_2\text{N}$ ($N:S = 0.73:0.27$, CDCl_3 solution) (a) Before heating, (b) after 1 day and (c) after 6 days of heating at 50°C .

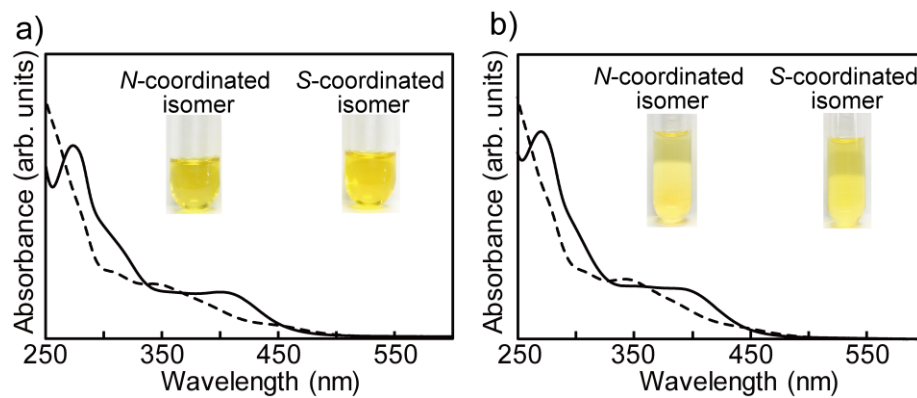


Figure S8. UV-Vis spectra and photographs of the *N*-coordinated (—) and *S*-coordinated (---) isomers in (a) dichloromethane and (b) methanol (concentrations: $80 \mu\text{mol L}^{-1}$).